AMERICAN ACADEMY OF OPHTHALMOLOGY®

Assessment of Retinal Volume in Individuals Without Ocular Disorders Based on Wide-Field Swept-Source OCT

Yoshiaki Chiku, MD, Takao Hirano, MD, PhD, Ken Hoshiyama, MD, Yasuhiro Iesato, MD, PhD, Toshinori Murata, MD, PhD

Purpose: To evaluate retinal volume (RV) in eyes without retinal disease using wide-field swept-source OCT (SS-OCT).

Design: Observational, cross-sectional design.

Participants: A total of 332 eyes of 166 healthy participants.

Methods: The eyes were imaged with OCT-S1 (Canon) using a protocol centered on the fovea cube scans (20 × 23 mm) of SS-OCT images. Retinal volume (6-mm circle, 6–20-mm ring) and various parameters were evaluated in a multivariate analysis using a generalized estimating equation model. Each quadrant of the macula except for the fovea (1–6 mm in diameter) and peripheral ring (6–20 mm in diameter) was also evaluated.

Main Outcome Measures: Retinal volume.

Results: In the multivariate analysis, older age and longer axial length were associated with smaller macular RV, whereas older age and left eye were associated with smaller peripheral RV. The temporal area was significantly smaller than all other areas in the macula (1–6 mm), whereas the inferior area was significantly smaller than all other areas in the peripheral retina (6–20 mm).

Conclusions: In wide-field SS-OCT images, age and left eye are negatively correlated with peripheral RV. The thinnest part of the retinal quadrant differs between the macular and peripheral retinas.

Financial Disclosure(s): Proprietary or commercial disclosure may be found in the Footnotes and Disclosures at the end of this article. *Ophthalmology Science 2024;4:100569* © *2024 by the American Academy of Ophthalmology. This is an open access article under the CC BY-NC-ND license (http://creativecommons.org/licenses/by-nc-nd/4.0/).*

Advancements in retinal imaging technology have transformed the understanding of retinal and choroidal diseases, enabling the detection of previously unseen abnormalities. With limited tissue penetration and relatively low resolution, first-generation time-domain OCT devices can only scan a small portion of the posterior pole.[1,2] Subsequent spectral-domain OCT technology has allowed for more precise visualization of the posterior pole anatomy and better visualization of deeper tissues.[3] Instead of the diode laser used in spectral-domain OCT, the recently introduced swept-source OCT (SS-OCT) uses a tunable wavelength light source. Swept-source OCT improves the penetration of the signal and allows the acquisition of large fields of view at higher scan speeds.[4] The newly developed SS-OCT Xephilio S1 (Canon) is capable of acquiring up to 23 × 20-mm wide-field OCT images in a single shot in a limited time (100 000 A-scans/s)[5] and provides an enhanced view from the vitreous to the sclera with improved penetration through media opacities.

The retina consists of 2 main parts: the macular and the peripheral. The macular retina is responsible for photopic vision, whereas the peripheral retina is responsible for scotopic vision. The peripheral retina plays an important role in movement detection and scene gist recognition to facilitate mobility, postural stability, and attention processing tasks.[6] Several ophthalmic diseases are characterized by morphological changes in the periphery, including retinitis pigmentosa, diabetic retinopathy, and uveitis.[7]

Spectral-domain OCT has revealed that macular volume is associated with age, sex, and axial length.[8,9] Spectralis OCT was used to evaluate peripheral retinal thickness in healthy young adults.[10] However, no such studies have been conducted using SS-OCT. This study aimed to investigate the possible association between retinal volume (RV) in the macula and peripheral retina and demographic and ocular anatomical characteristics using SS-OCT.

Methods

Study Design and Participants

This prospective study was conducted at Shinshu University between March 2020 and December 2022. We included healthy volunteers with no visual symptoms or history of ocular disease. The following 5 exclusion criteria were applied: (1) presence of current or previous vitreoretinal–choroidal disease, (2) hyperopia >3.0 diopters (D) or myopia >5.0 D, (3) axial length >26.5 mm, (4) previous ocular surgery other than cataract surgery, and (5)

https://doi.org/10.1016/j.xops.2024.100569
ISSN 2666-9145/24

ocular media opacity affecting the image quality. This study was conducted in accordance with the Declaration of Helsinki and approved by the Institutional Review Board of Shinshu University School of Medicine (approval number 4908). All participants or their parents/guardians, if aged <20 years, provided informed consent prior to participation in this study.

Study Equipment and Procedures

All OCT examinations were performed using an SS-OCT camera (Xephilio OCT-S1; Canon) by trained examiners with no pupil dilation. The instrument had a scan width of 23 mm and a field of view of 78°. The data were acquired at a frequency of 100 kHz with an optical axial resolution of 8 μm and a lateral resolution of 30 μm. B-scans measuring 23 mm × 5.3 mm were acquired for each eye of the participants. In addition, 23 mm × 20 mm (1024 × 128 A-scans) cube scans centered on the fovea were acquired from both eyes of each participants. The wavelength of the light source was set to 1010 to 1110 nm. The spherical equivalent refraction and axial length were measured using a built-in refractometer within the SS-OCT. During the examination, the participants were instructed to fixate on an internal fixation target provided by the SS-OCT with the examined eye. The centering of scans was confirmed by a fundus camera integrated with the instrument.

Data Collection

All scans were reviewed for quality and signal strength. Scans with motion artifacts or with a signal strength <7 were excluded from the analysis. To generate the color-coded en face retinal thickness map, the SS-OCT images were further analyzed using an OCT extractor (Canon) and an OCT map viewer. The inner border of the internal limiting membrane and the outer border of the retinal pigment epithelium were automatically detected. Automatic segmentations of the retina were reviewed by 2 experienced retina physicians (Y.C. and T.H.), and manual corrections were performed if the automated segmentations were deemed inaccurate. Consensus segmentation was reached in all cases. The color-coded en face retinal thickness map was then created to show the distance between the 2 detected boundaries of the internal limiting membrane and retinal pigment epithelium lines. To study the regional distribution of RV from a 23 × 20-mm scan, we created a grid composed of 1-, 6-, and 20-mm circles centered on the fovea. This grid divided the retina area further into superior, inferior, temporal, and nasal quadrants, but the central 1-mm circle was used in its entirety without quadrants (Fig 1). The thicknesses of all measurement points within each of the 13 areas based on the grid were averaged, enabling us to determine the mean sectorial retinal thickness. Further, on the basis of the retinal thickness obtained, we calculated the RV within each sector in the grid. The area of each sector was determined mathematically, and the following values were used:

Area of the central subfield: 0.7854 mm^2.

Area of the subfields of each macular ring (superior, inferior, temporal, and nasal): 6.8722 mm^2.

Area of the subfield of each peripheral ring (superior, inferior, temporal, and nasal): 71.4712 mm^2.

The volume of each sector was determined as follows.

Volume of each sector = Mean thickness of each sector * Area of each sector.

The macular and peripheral ring volumes were defined as the sum of the superior, inferior, nasal, and temporal sectors. The map viewer displayed the percentage of the retina measured as a valid area ratio in each subfield. All patients with a valid retinal area ratio of <80% were excluded. Two experienced retinal specialists (Y.C. and T.H.) independently reviewed the SS-OCT B-scan images and determined the posterior vitreous detachment status. Complete posterior vitreous detachment was defined as the absence of adhesion between the retina and posterior vitreous cortex. The brightness and contrast were adjusted by grader preference at the time of evaluation. Disagreements were resolved via discussions.

Statistical Analyses

Statistical analyses were performed using the Statistical Package for the Social Sciences version 29.0 software (SPSS Inc). Statistical significance was defined as a P value <0.05. The association between the RV (macular retina, peripheral retina) and other variables was assessed using a generalized estimating equation analysis with an exchangeable correlation structure to account for the inclusion of 2 eyes from a single individual. Except for the multivariate analysis, we evaluated the participants' average RV obtained from the RV of the right and left eyes. In the univariate analysis, we used the Kruskal–Wallis test to assess the differences among the age groups. The association between the quantitative variables was assessed using Spearman's correlation coefficient.

Results

Baseline Characteristics

Overall, 332 eyes of 166 participants (101 females, 65 males) with a mean age of 43.3 ± 26.0 (range, 4–89) years were evaluated. Table 1 shows the baseline characteristics of the participants. The mean axial length was 24.6 ± 1.0 mm. Complete posterior vitreous detachment was observed in 92 (27.7%) eyes. In total, 234 (70.5%) eyes were classified as low myopia (≥−5 and <−1 D), 77 (23.2%) as emmetropia, and 21 (6.3%) as low hyperopia (>+1 D and ≤+3 D).

Generalized Estimating Equation and Univariate Analyses

The RVs were 8.7 ± 0.4 and 8.7 ± 0.4 mm^3 in the right and left macular retinas, respectively, and 65.7 ± 2.7 and 65.6 ± 2.8 mm^3 in the right and left peripheral retinas, respectively. We evaluated the association between RV and participants' characteristics using generalized estimating equation. We observed statistically significant associations between the macular RV and age ($P < 0.001$) and axial length ($P = 0.024$) in the multivariate analysis. We found statistically significant associations between the peripheral RV and age ($P < 0.001$) and left eye ($P = 0.017$) in the multivariate analysis (Table 2). In the univariate analysis, the RV significantly differed among the age groups ($P <$ 0.0001 in both eyes in the macular RV, $P < 0.01$ in both eyes in the peripheral RV, Kruskal–Wallis test) (Fig 2). A longer axial length was associated with the smaller peripheral RV ($R = -0.08$, $P = 0.25$, macular RV; $R = -0.25$, $P = 0.0011$, peripheral RV; Spearman's correlation test) (Fig 3).

In the macula, the nasal quadrant had the largest RV (2.233 ± 0.114 mm^3), followed by the superior (2.137 ± 0.104 mm^3), inferior (2.057 ± 0.103 mm^3), and temporal (2.034 ± 0.099 mm^3) quadrants (Fig 4). In the peripheral retina, the nasal quadrant had the largest RV (18.4 ± 0.9 mm^3), followed by the superior (16.4 ± 0.6

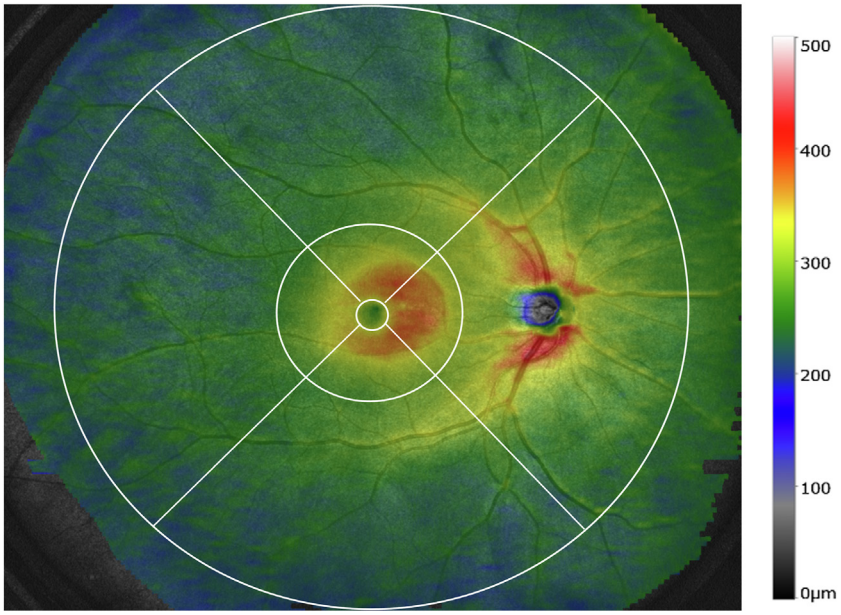

Figure 1. Color map of the application of the original circle grid to the retinal thickness. We developed a grid with diameters of 1, 6, and 20 mm; the macular retina without the fovea and peripheral retina were enclosed by circles with diameters of 1 and 6 mm and 6 and 20 mm, respectively, which were divided into 4 subfields: superior, inferior, nasal, and temporal.

mm^3), temporal (15.5 ± 0.6 mm^3), and inferior (15.2 ± 0.6 mm^3) quadrants (Fig 4).

Discussion

This study aimed to investigate the association between macular and peripheral RVs and the demographic and anatomical characteristics of individuals with healthy eyes. To the best of our knowledge, no systematic study has been conducted on healthy peripheral RV using SS-OCT. We included both eyes in our analysis and used generalized estimating equation to account for within-individual correlations. Our results showed a statistically significant association between age and axial length and the macular RV, whereas age and laterality were significantly associated with the peripheral RV. These results suggest that age and axial length are important factors in the assessment of RV.

Table 1. Baseline Characteristics of the Subjects

Characteristics	Data
Age (years)	
Mean ± standard deviation	43.3 ± 26.0
Range	4–89
Sex, n (%)	
Female	101 (60.8%)
Male	65 (39.2%)
Eye (n, %)	
Right	166 (50%)
Left	166 (50%)
Axial length (mm)	
Mean ± standard deviation	24.6 ± 1.0
Range	21.7–26.5
Complete PVD (n, %)	
Present	92 (27.7%)
Absent	240 (72.3%)
Refractive error category, n (%)	
Low myopia (≥−5 and <−1 D)	234 (70.5%)
Emmetropia (≥−1 and ≤+1 D)	77 (23.2%)
Low hyperopia (>+1 D and ≤+3 D)	21 (6.3%)

D = diopters; PVD = posterior vitreous detachment.
Data on age and sex are listed for subjects, and data on axial length, complete PVD, and refractive error category are listed for eyes.

A previous study reported that age had no significant effect on peripheral retinal thickness; however, that study included only a narrow age range of 19 to 30 years.[10] In contrast, the present study included a wide age range of 4 to 89 years and found that age was significantly associated with RV. Although the effect of age on macular thinning has been well documented,[11] this study reports age-related thinning in the peripheral retina, which has not been extensively explored in previous literature.

In the healthy population, we found significant differences in RV with age. This is consistent with previous reports on retinal layer thickness. The retinal nerve fiber layers, axons, and ganglion cell layers are particularly susceptible to loss with age.[12,13] Another study suggested that the thicknesses of the retinal nerve fiber layer, ganglion cell layer, inner plexiform layer, inner nuclear layer, and photoreceptor inner segment were negatively correlated with age.[14] As the autosegmentation system in OCT-S1 cannot evaluate the peripheral retina, we could not assess each retinal layer. Therefore, further studies on the peripheral retinal layer are warranted.

We showed that the peripheral retina was significantly smaller in the left eye than in the right eye. However, the

Table 2. The Univariate and Multivariate Generalized Estimating Equation Analyses of the Association Between RVs and Baseline Characteristics

		Macular RV (0–6 mm)				Peripheral RV (6–20 mm)			
		Univariate		*Multivariate*		*Univariate*		*Multivariate*	
Variable	**Category**	*β (SE)*	P	*β (SE)*	P	*β (SE)*	P	*β (SE)*	P
Age		−0.16 (0.02)	<0.001	−0.13 (0.03)	<0.001	−0.92 (0.19)	<0.001	−0.93 (0.22)	<0.001
Sex	Female	−0.05 (0.03)	0.082	−0.10 (0.05)	0.079	−0.17 (0.20)	0.392	−0.29 (0.39)	0.467
	Male	Ref							
Laterality	Left	0.00 (0.00)	0.570	0.00 (0.01)	0.842	−0.09 (0.04)	0.027	−0.20 (0.08)	0.017
	Right	Ref							
Complete PVD	Absent	0.10 (0.02)	<0.001	0.09 (0.06)	0.142	0.29 (0.13)	0.030	−0.01 (0.33)	0.959
	Present	Ref							
Axial length		−0.03 (0.01)	0.09	−0.04 (0.01)	0.024	−0.03 (0.10)	0.743	−0.09 (0.10)	0.388

PVD = posterior vitreous detachment; ref = reference; RV = retinal volume; SE = standard error.
β is standardized.

results should be interpreted with caution. In our examination protocol, we first examined the right eye, which may have affected our results. That is, the patient may have lost concentration, and the image quality may have been affected by eye or head movements when the left eye was examined. Previous studies have also suggested that the order in which the right and left eyes are examined may affect results.[15] Further studies are required to evaluate the difference between the right and left eyes, as previous studies on choroidal thickness[16] and retinal ganglion cell layer

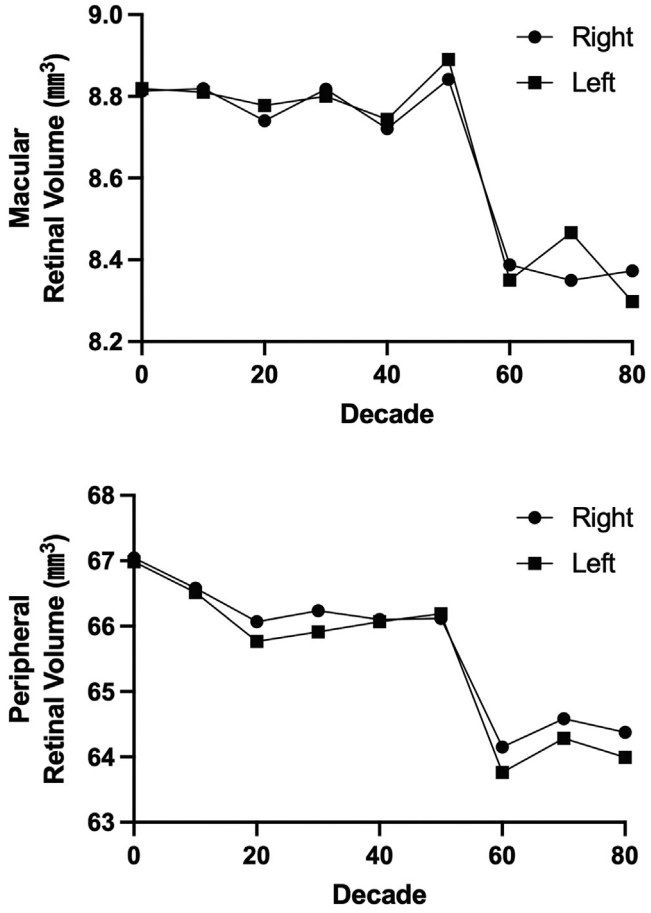

Figure 2. Association between age and retinal volume (RV). The RV significantly differed among the age groups ($P < 0.001$ in both eyes in the macula RV, $P < 0.01$ in both eyes in the peripheral RV).

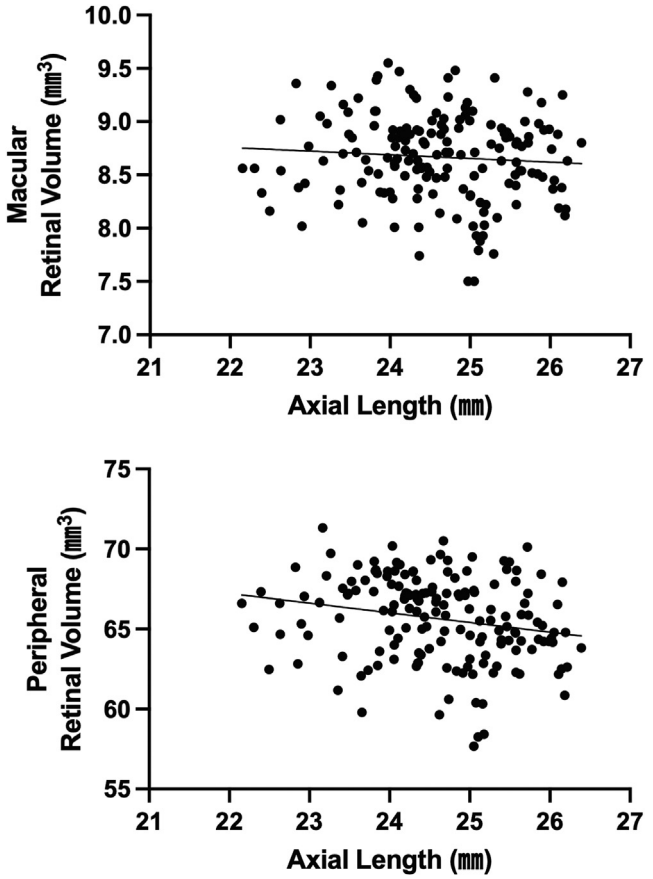

Figure 3. Association between axial length and retinal volume (RV). A longer axial length was associated with the smaller peripheral RV (R = −0.09, $P = 0.25$, macular RV; R = −0.25, $P = 0.0011$, peripheral RV).

thickness[17] have not reported any differences between the left and right eyes.

Several studies have reported an association between the axial length and RV. For example, a previous study found that a long axial length was associated with decreased overall macular thickness and macular volume.[9] Our results also support this association, as we found a significant association between axial length and macular RVs in multivariate analysis.

However, the association between the axial length and macular thickness remains controversial. The myopic enlargement of the globe is mainly due to axial elongation, whereas the horizontal and vertical diameters increase only slightly.[18,19] Jost et al also found that axial elongation in

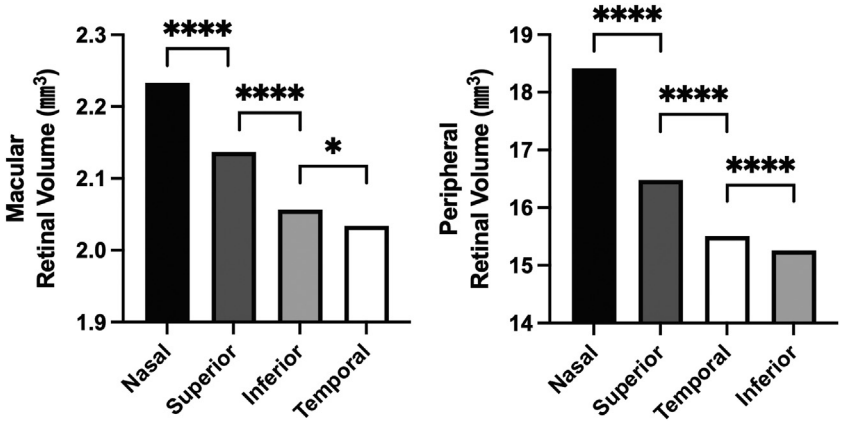

Figure 4. Retinal volume in each subfield in the macula without the fovea (1−6 mm) and the peripheral retina (6−20 mm). *$P < 0.05$. ****$P < 0.0001$. Dunn's multiple comparison test.

myopia was associated with retinal thinning in the equatorial and pre-equatorial regions, whereas foveal retinal thickness was largely unaffected.[20] Further studies are required as differences in research methods, participants' backgrounds, and consideration of reflection- and axial length-induced magnification effects may have led to differences in these study results.

This study investigated the thinnest regions of the retina in both the macula and periphery. Our results indicate that the thinnest retina was located in the temporal region of the macula. This finding is consistent with that of a previous study showing that the thinnest retinas are temporally located in the macula.[8]

To the best of our knowledge, this is the first study to demonstrate that the inferior sector is the thinnest in the peripheral retina. Although the exact reasons for the observed differences in the retinal thickness remain unclear, several hypotheses have been proposed. One possibility is a difference in blood supply. Blood supply correlates with retinal thickness, and an earlier study elucidated that the outer retina and choroidal thickness were correlated in the entire macula.[21] In a previous study, the peripheral choroid was reported to be the thinnest in the inferonasal area.[22] The inferior region of the peripheral retina may have a thinner retinal layer because of the relatively reduced blood supply compared with other regions.

Differences in the importance of the visual field should also be considered. For example, safe driving necessitates a well-functioning inferior field because most external action occurs here.[23] The inferior peripheral retina may be less important than the superior peripheral retina, leading to a thinner anatomical structure of the inferior retina. However, these hypotheses do not explain why the inferior retina is the thinnest, requiring further investigation. Future studies should further explore these hypotheses and uncover other factors that may contribute to the observed differences in retinal thickness.

This study has some limitations. First, the incident light on the retina was not perpendicular to the retina as it moved toward the periphery, which may have resulted in measurement errors. In future studies, it will be important to correct this error to ensure more accurate results. Second, images from the long axial eye lengths cover more peripheral regions compared with those acquired from short axial eyes, even if the same scan protocols are used. This could have significantly overestimated the statistical significance of the association between peripheral RV and axial eye lengths. Since the Canon OCT-S1 could not correct the ETDRS circle diameter using the Littmann's formula, it is necessary to consider the magnification effect due to axial length. Third, the male/female ratio was inconsistent for each age group, which may have influenced the multivariate analysis. Future studies should consider balancing the male/female ratio to avoid potential biases. Fourth, because the OCT-S1 device used in this study is only available in Japan and some parts of Europe, Korea, Taiwan, and Singapore, the study population comprised only Japanese participants. Therefore, multiethnic studies are required to evaluate the usefulness of OCT-S1 in different regions. Finally, the inclusion of eyes that underwent cataract surgery is another limitation that must be considered. We acknowledge the potential effects of the history of cataract surgery on the results.

Despite these limitations, our study results showed a significant association between the peripheral RV and age and laterality. In addition, our results confirm that the inferior retina is the thinnest part of the peripheral retina. The current study adds to the growing body of literature on the use of OCT-S1 for the assessment of retinal parameters and highlights the need for further studies to address the limitations of this study.

Availability of Data

The research data are confidential.

Acknowledgments

The authors would like to thank Editage (www.editage.com) for English language editing.

Footnotes and Disclosures

Originally received: January 22, 2024.
Final revision: May 29, 2024.
Accepted: June 11, 2024.
Available online: June 21, 2024. Manuscript no. XOPS-D-24-00022.

Department of Ophthalmology, Shinshu University School of Medicine, Matsumoto, Nagano, Japan.

Disclosure(s):

All authors have completed and submitted the ICMJE disclosures form.

The author(s) have made the following disclosure(s):

T.H.: Personal fees — Novartis Pharma K.K., Bayer, Canon, Kowa Pharmaceutical, Senju Pharmaceutical, Chugai Pharmaceutical, Carl Zeiss Meditec.

T.M.: Personal fees — Novartis Pharma K.K., Bayer, Canon, Kowa Pharmaceutical, Senju Pharmaceutical, Chugai Pharmaceutical, Kyowa Kirin, Carl Zeiss Meditec.

This work was supported by the 2022 Shinshu University Basic Research Support Project (T.H.). The funding organization had no role in the design or conduct of this research. This work was also supported by Japanese Grants-in-Aid for Scientific Research (KAKENHI) Grant Number 24K12759.

No animal subjects were used in this study.

HUMAN SUBJECTS: Human subjects were included in this study. This study was conducted in accordance with the Declaration of Helsinki and approved by the Institutional Review Board of Shinshu University School of Medicine (approval number 4908). All participants or their parents/guardians, if aged <20 years, provided informed consent prior to participation in this study.

Author Contributions:

Conception and design: Chiku, Hirano

Data collection: Chiku, Hirano

Analysis and interpretation: Chiku, Hirano, Hoshiyama, Iesato, Murata

Obtained funding: N/A. Study was performed as part of regular employment duties at Shinshu University, Japan. No additional funding was provided.

Overall responsibility: Chiku, Hirano, Hoshiyama, Iesato, Murata

Presented at the 127th Annual Meeting of the Japanese Ophthalmological Society, Tokyo, Japan, held from April 6−9, 2023. Presented at the 2023 Annual Meeting of the Association for Research in Vision and Ophthalmology, New Orleans, Louisiana, held from April 23−27, 2023.

Abbreviations and Acronyms:
D = diopters; **RV** = retinal volume; **SS-OCT** = swept-source OCT.

Keywords:
Macula, Peripheral retina, Retinal volume, Swept-source OCT.

Correspondence:
Takao Hirano, MD, PhD, Department of Ophthalmology, Shinshu University School of Medicine, 3-1-1 Asahi, Matsumoto, Nagano 390-8621, Japan. E-mail: takaoh@shinshu-u.ac.jp.

References

1. Huang D, Swanson EA, Lin CP, et al. Optical coherence tomography. *Science*. 1991;254:1178−1181.
2. Drexler W, Morgner U, Ghanta RK, et al. Ultrahigh-resolution ophthalmic optical coherence tomography. *Nat Med*. 2001;7:502−507.
3. De Boer JF, Cense B, Park BH, et al. Improved signal-to-noise ratio in spectral-domain compared with time-domain optical coherence tomography. *Opt Lett*. 2003;28:2067−2069.
4. Adhi M, Duker JS. Optical coherence tomography–current and future applications. *Curr Opin Ophthalmol*. 2013;24:213−221.
5. Chiku Y, Hirano T, Takahashi Y, et al. Evaluating posterior vitreous detachment by widefield 23-mm swept-source optical coherence tomography imaging in healthy subjects. *Sci Rep*. 2021;11:19754.
6. Quinn N, Csincsik L, Flynn E, et al. The clinical relevance of visualizing the peripheral retina. *Prog Retin Eye Res*. 2019;68:83−109.
7. Kumar V, Surve A, Kumawat D, et al. Ultra-wide field retinal imaging: a wider clinical perspective. *Indian J Ophthalmol*. 2021;69:824−835.
8. Pokharel A, Shrestha GS, Shrestha JB. Macular thickness and macular volume measurements using spectral domain optical coherence tomography in normal Nepalese eyes. *Clin Ophthalmol*. 2016;10:511−519.
9. Song WK, Lee SC, Lee ES, et al. Macular thickness variations with sex, age, and axial length in healthy subjects: a spectral domain-optical coherence tomography study. *Invest Ophthalmol Vis Sci*. 2010;51:3913−3918.
10. Wenner Y, Wismann S, Preising MN, et al. Normative values of peripheral retinal thickness measured with Spectralis OCT in healthy young adults. *Graefes Arch Clin Exp Ophthalmol*. 2014;252:1195−1205.
11. Eriksson U, Alm A. Macular thickness decreases with age in normal eyes: a study on the macular thickness map protocol in the Stratus OCT. *Br J Ophthalmol*. 2009;93:1448−1452.
12. Gao H, Hollyfield JG. Aging of the human retina. Differential loss of neurons and retinal pigment epithelial cells. *Invest Ophthalmol Vis Sci*. 1992;33:1−17.
13. Nag TC, Wadhwa S. Ultrastructure of the human retina in aging and various pathological states. *Micron*. 2012;43:759−781.
14. Ooto S, Hangai M, Tomidokoro A, et al. Effects of age, sex, and axial length on the three-dimensional profile of normal macular layer structures. *Invest Ophthalmol Vis Sci*. 2011;52:8769−8779.
15. Sugawara A, Kato K, Nagashima R, et al. Effects of recording sequence on flicker electroretinographics recorded with natural pupils corrected for pupil area. *Acta Ophthalmol*. 2021;99:411−417.
16. Gyawali P, Kharel Sitaula R, Kharal A, et al. Sub-foveal choroidal thickness in healthy Nepalese population. *Clin Optom (Auckl)*. 2019;11:145−149.
17. Al-Hawasi A, Lagali N. Retinal ganglion cell layer thickness and volume measured by OCT changes with age, sex, and axial length in a healthy population. *BMC Ophthalmol*. 2022;22:278.
18. Vurgese S, Panda-Jonas S, Jonas JB. Scleral thickness in human eyes. *PLoS One*. 2012;7:e29692.
19. Moriyama M, Ohno-Matsui K, Hayashi K, et al. Topographic analyses of shape of eyes with pathologic myopia by high-resolution three-dimensional magnetic resonance imaging. *Ophthalmology*. 2011;118:1626−1637.
20. Jonas JB, Xu L, Wei WB, et al. Retinal thickness and axial length. *Invest Ophthalmol Vis Sci*. 2016;57:1791−1797.
21. Maruko I, Arakawa H, Koizumi H, et al. Age-dependent morphologic alterations in the outer retinal and choroidal thicknesses using swept source optical coherence tomography. *PLoS One*. 2016;11:e0159439.
22. Funatsu R, Sonoda S, Terasaki H, et al. Normal peripheral choroidal thickness measured by widefield optical coherence tomography. *Retina*. 2023;43:490−497.
23. Dow J. Visual field defects may not affect safe driving. *Traffic Inj Prev*. 2011;12:483−490.